

Free-Standing Carbon Nanotube Films as Optical Accumulators for Multiplex SERRS Attomolar Detection

Paula Aldeanueva-Potel, Miguel A. Correa-Duarte, Ramón A. Alvarez-Puebla,* and Luis M. Liz-Marzán

Departamento de Química Física and Unidad Asociada CSIC, Universidade de Vigo, 36310 Vigo, Spain

ABSTRACT A novel hybrid material comprising silver aggregates supported on the porous structure of a free-standing carbon nanotube film was devised and fabricated. This material readily allows filtration of large volumes of fluids, while retaining the active analytes on silver aggregates so that their characteristic surface-enhanced resonance Raman scattering signals could be registered. The direct identification of multiple analytes at the attomolar regime was readily achieved through their single-molecule spectra.

KEYWORDS: silver nanoparticles • CNTs • films • hot spots • SERS • ultradetection

INTRODUCTION

Surface-enhanced resonance Raman scattering (SERRS) has been identified as one of the most powerful and versatile analytical tools, with detection limits down to the single molecule at ambient conditions (1, 2). However, such impressive detection capabilities appear so far to be academic exercises rather than a practical tool for analytical detection. The vast majority of the literature dealing with ultrasensitive detection via SERS/SERRS consistently avoids the term “molar”, substituting it with “mole regime”. That is because while zeptomol (10^{-21} mol) and single-molecule (SM) detection have been successfully reported (3–7), the experimental conditions under which these experiments are to be carried out require the use of highly concentrated analyte solutions. For example, in a typical experiment, the SM regime is achieved when, statistically, the number of molecules sampled with the laser per unit area is approximately 1. Under such conditions and working with a $50\times$ objective (NA 0.75), which provides a spatial resolution of about $1\ \mu\text{m}^2$, SM detection is achieved when $10\ \mu\text{L}$ of a 10^{-11} M analyte solution is homogeneously distributed on a $1\ \text{cm}^2$ surface. In the case of zeptomol (10^{-21}) or attomol (10^{-18}) detection, only 10^{-9} or 10^{-6} M solutions are required, respectively (8–12). That is academically considered to be sufficient for demonstrating SM/zeptomol/attomol detection limits; however, regarding common analytical applications, this technique has very limited applicability.

We present here the design and fabrication of a composite material based on silver nanoparticle (AgNP) aggregates supported on a free-standing carbon nanotube (CNT) multilayer film. In this system, CNTs provide a porous support with high mechanical strength to retain the optically active

aggregates on the upper part of the filter while avoiding blocking of the filter pores and thus allowing a relatively fast flow of large sample volumes. Additionally, this material can be easily peeled away from its original substrate and subsequently supported on other surfaces of interest. Optical-enhancing properties and analytical applicability of the material are demonstrated by a simultaneous determination of two analytes at the attomolar (aM) level.

EXPERIMENTAL METHODS

Materials. Unless otherwise is stated, all of the chemicals were purchased from Sigma-Aldrich. Glassware was cleaned with aqua regia and extensively washed with water. Milli-Q water (Millipore) was used throughout all of the experiments.

CNT Polyelectrolyte Functionalization. Multiwalled CNTs (Nanolab) were redispersed in ultrapure water ($18\ \text{M}\Omega\ \text{cm}$), as previously described (13, 14). Briefly, CNTs were dispersed in a 1 wt % aqueous solution of polyallylamine hydrochloride (PAH) up to a concentration of 150 mg/L. A combination of rapid stirring and sonication was used to ensure the presence of well-dispersed, individual nanotubes. Excess PAH was removed by repeated centrifugation and redispersion cycles.

AgNPs. AgNPs were synthesized by the addition of 2 mL of a sodium citrate solution (1%) to 100 mL of a 10^{-3} M boiling aqueous solution of Ag^+ under continuous stirring. After 30 min, the resulting colloids show a turbid gray-green color with a localized surface plasmon resonance at 412 nm.

Filter Fabrication. A suspension containing CNT@PAH (5 mL, 0.045 mg/mL) was injected into a commercial cellulose acetate syringe filter (filter diameter, 25 mm; pore diameter, $0.45\ \mu\text{m}$; ALBET). Then, the filter was separated from its plastic support, dried at $60\ ^\circ\text{C}$, and immersed in a 50 mL beaker filled with the AgNP suspension. AgNPs were aggregated and precipitated by the addition of 2 mL of 0.1 M NaCl to the suspension. After that, the filter was carefully lifted and dried again at $60\ ^\circ\text{C}$. The rest of the work was carried out on filters on their original support (cellulose acetate). To demonstrate the free-standing properties of the filters, one of them was removed from the cellulose acetate matrix by immersing it in acetone and placing it onto an analytical glass microfiber filter (Whatman).

Material Characterization. Optical characterization was carried out by UV/vis/near-IR spectroscopy with a Cary 5000 spectrophotometer. Scanning electron microscopy (SEM) im-

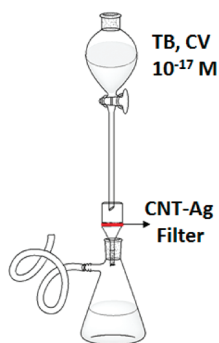
* Author to whom correspondence should be addressed. E-mail: ramon.alvarez@uvigo.es.

Received for review December 9, 2009 and accepted December 30, 2009

DOI: 10.1021/am9008715

© 2010 American Chemical Society

Scheme 1. Cellulose–CNT–Ag Setup for Ultradetection in Large Sample Volumes



ages were obtained with a JEOL JSM 6700F field-emission microscope. A dedicated backscattered electron detector (Aurata YAG) was used to enhance the signal from silver particles. A cross section of the filter was studied with SEM after preparation by the lift-out technique in a FIB workstation with a FEI Helios 400 NanoLab dual-beam microscope. To protect the delicate surface features of the sample, it was coated with a thin layer of carbon prior to platinum coating and thinning (15).

SERS Ultradetection. SERS ultradetection experiments were carried out in a setup as sketched in Scheme 1. A filter was placed on a Buchner funnel under vacuum. In order to set an active filtration area of 1 cm², the rest of the filter was passivated with Teflon tape. Then different volumes (from 10 μL to 1 L) of a 10⁻¹⁷ M solution of crystal violet (CV) and toluidine blue (TB) were each passed through it from a 1 L separation funnel (note that after 1 L of a 10⁻¹⁷ M solution was passed through, the following experiments were carried out with 1 L each of 10⁻¹⁶ and 10⁻¹⁵ M solutions). The drop speed was set to have time to pass through 1 cm² of the filter area before the next drop, with an approximated filtering speed of 200 mL/h. After each addition, the filter was analyzed by SERS with a Renishaw Invia Reflex system equipped with Peltier charge-coupled device detectors and a Leica confocal microscope. The spectrograph used high-resolution gratings with additional band-pass filter optics. Samples were studied by mapping areas of 61 × 101 μm², with a step size of 2.5 μm (1025 spectra each) with a 633 nm laser line (200 ms and 10 mW of power at the sample). The laser was focused on the sample by using a 50× objective (NA 0.75), providing a spatial resolution of 1 μm².

RESULTS AND DISCUSSION

Parts a–d of Figure 1 show optical images illustrating the fabrication process of the CNT–Ag filter. The CNT supporting film was assembled by injection of CNT@PAH into a commercial syringe filter (Figure 1a). Upon drying, a CNT film that was supported on the filter cellulose membrane (Figure 1b) was obtained. AgNPs were deposited on the upper face by simply immersing the cellulose–CNT filter in a standard silver citrate colloid, followed by NP aggregation and precipitation induced by NaCl addition (16). This yields a material (cellulose–CNT–Ag) with a high density of hot spots (6, 17, 18) (Figures 1e and 2) supported on the porous CNT film (Figures 1f and 2). Localized surface plasmon resonances of a silver film prepared under the same conditions on a glass slide (Figure 3a) show the characteristic features of extensively aggregated AgNPs. Cutting a slice of the cellulose–CNT filter by means of focused ion beam (FIB) lithography allowed high-resolution cross-sectional SEM imaging (15) (Figures 1g and 2), clearly showing a distribu-

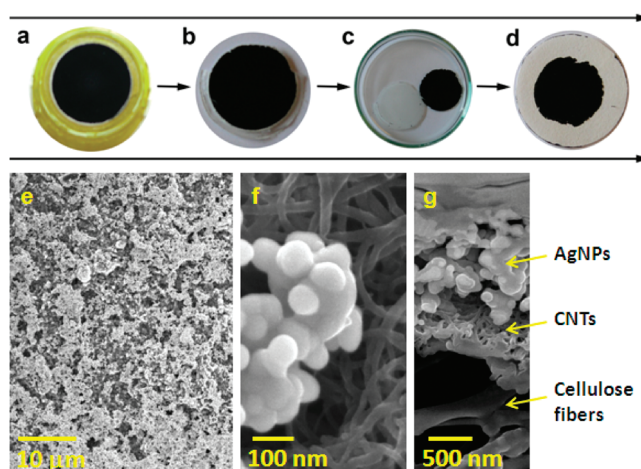


FIGURE 1. Cellulose–CNT–Ag filter before (a) and after (b) separation of the plastic support. CNT–Ag filter after separation of the cellulose matrix by immersing the material in acetone (c) and supported on a glass fiber filter (d). SEM images of the surface of the cellulose–CNT–Ag and of the structure of the hot spots formed by the AgNPs on the CNT film surface. (e and f). Cross-sectional SEM image of the filter after FIB preparation (g).

tion of the three components: silver aggregates, which act as the optically active element; CNT supporting layers, which not only acts as a mechanically robust support for AgNPs but also prevents blocking of the filter porosity. Additionally, the cellulose matrix provides a solid, porous support for the filter, adding extra mechanical resistance to the material. It should be noted that while, in this letter, we used the cellulose–CNT–Ag filter as prepared, the CNT–Ag is self-supporting and can be easily removed from the cellulose matrix by immersing it in acetone (Figure 1c). Thus, the CNT–Ag film can be used either as is or supported on a different matrix of interest, such as a glass fiber filter (Figure 1d).

The SERS/SERRS multiplex ultrasensitive analytical application is based on the assumption that, for extremely diluted solutions, detection can be achieved when a sufficient number of analyte molecules—just one for molecules with large SERS/SERRS cross sections—are retained at a highly efficient optical hot spot on the sampled surface. With such a scheme in mind, the only requisite for detecting whatever concentration of a given analyte would simply require flow of enough volume of the sample through the filter until accumulating a sufficient number of molecules to register its SERS/SERRS spectrum. Thus, to prove this statement, we prepared an aqueous solution containing two blue dyes, CV and TB, with a concentration of 10⁻¹⁷ M (10 aM) in each species. Both CV and TB are resonant upon excitation with a 633 nm laser line (Figure 3b), and SERRS spectra (Figure 3c) can be measured when they are in contact with nanostructured silver or gold.

Different volumes (10 μL to 1 L) of the dilute dye solution (10⁻¹⁷ M) were flowed through the cellulose–CNT–Ag filter by using the setup described in the Experimental Methods (Scheme 1). After each addition, the filter was dried and mapped using a 633 nm laser line focused with a 50× objective (1025 spectra). For the smallest volumes (10 μL, 100 μL, and 1 mL), no signal was recorded (Figure 4). This

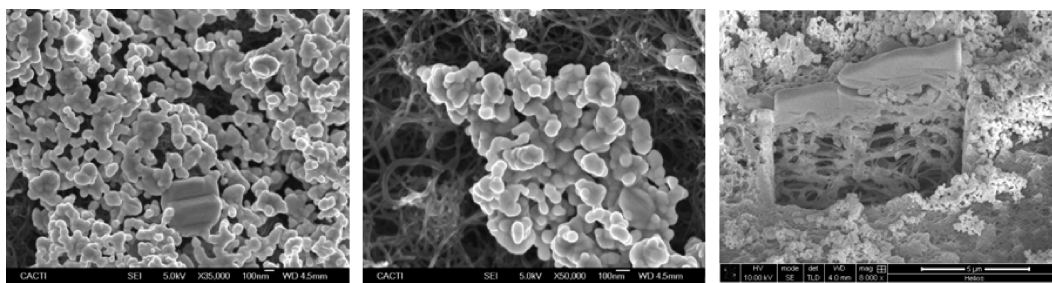


FIGURE 2. SEM images of the cellulose–CNT–Ag filter, detailing the hot spot structure and the FIB preparation.

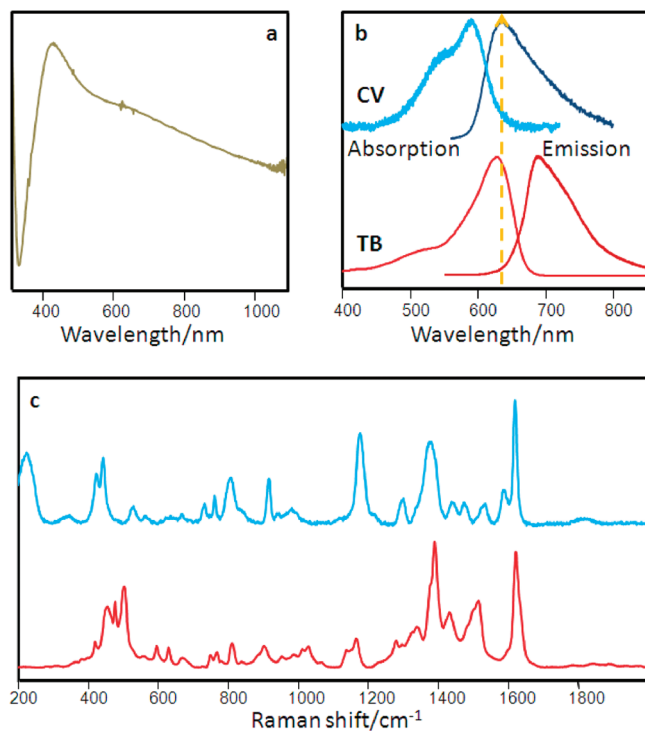


FIGURE 3. (a) UV/vis spectrum of a similarly aggregated AgNP film on glass. (b) Electronic absorption and emission spectra of CV and TB. (c) Ensemble SERRS spectra of CV (blue) and TB (red).

could be expected because the estimated densities of the molecules per square micrometer are 10^{-6} , 10^{-5} , and 10^{-4} , respectively. However, when 10 mL is flowed, the spectrum of CV was registered at certain spots. Even though the density of the molecules is still as low as $10^{-5} \mu\text{m}^{-2}$, over 1000 spots were mapped, so that statistically at least one molecule should be present in the studied area. No signal was identified for TB because highly active hot spots are randomly distributed through the surface (19, 20), and the molecule might not be attached to one of them. This was confirmed by mapping a larger surface, where indeed TB spectra were registered (Figure 5). After filtration of 100 mL, four active spots were identified for CV and three for TB (10 were expected from statistics). As in the former case, all of the spectra are characteristic for a single molecule, with slight signal fluctuations, i.e., changes in the frequency, bandwidth, and relative intensity (21). When 1 L of the sample was filtered, the amount of active spots significantly increased for both analytes (37 and 20 for CV and TB, respectively). In addition, some spots (6) were recorded with vibrational features of both dyes, which confirms that the

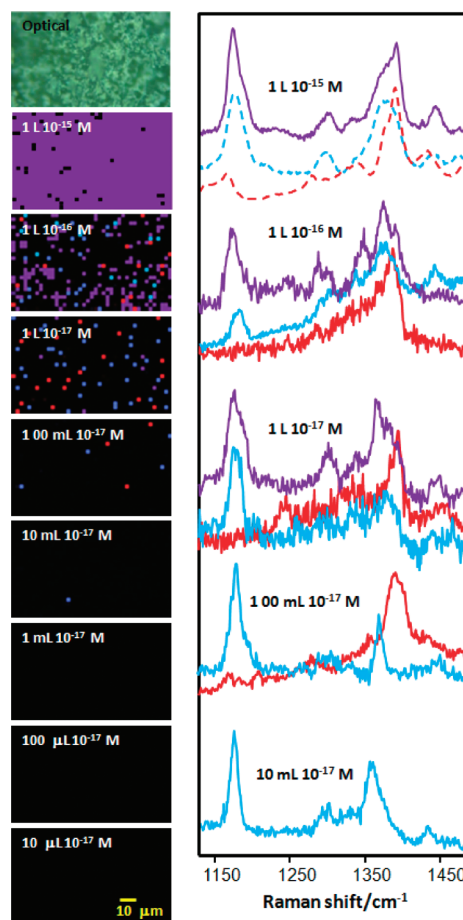


FIGURE 4. SERRS spectra (right) and mapping (left) of the cellulose–CNT–Ag filter after filtering it through different volumes of CV and TB solutions. Dotted spectra correspond to the reference ensemble SERRS spectra of CV or TB. Color code: blue, CV; red, TB; purple, CV + TB.

previous measurements (10 and 100 mL) correspond indeed to SM–SERRS spectra (22). For concentrated samples (1 L, 10^{-15} M), the spectra recorded at almost every spot of the surface revealed the presence of both analytes. Additionally, those spectra may be ascribed to a collection of molecules because they perfectly fit with the ensemble SERRS spectra of “concentrated” solutions of CV and TB (dotted spectra in Figure 4). In fact, this breakdown between the SM regime and the ensemble spectra of the analytes was detected for concentrations of around 100 molecules/ μm^2 , as previously reported (19, 22–24).

To summarize, we fabricated a hybrid material comprising highly active silver aggregates supported on the porous structure of a free-standing CNT film. This material allows

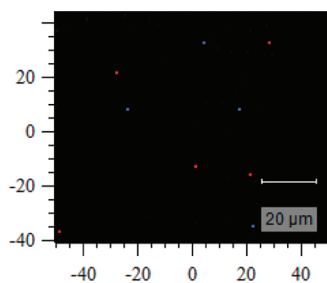


FIGURE 5. Map of a larger area ($91 \times 85 \mu\text{m}$ with a step size of $1 \mu\text{m}$, 7735 spectra) of cellulose–CNT–Ag after filtering 10 mL of a 10^{-17} M solution in TB and CV. Blue (CV) or red (TB) spots confirm the SM events for both analytes.

for the easy and fast filtration of large volumes of fluids. While the CNT film acts as a supporting structure preventing silver aggregates from blocking the filter, AgNPs act as the optically active sensor element for SERS. As the sample flows, silver aggregates retain the active analytes, so that their characteristic Raman-enhanced signals can be recorded at attomolar concentrations. Moreover, by filtering small volumes of very dilute concentrations, the filter registers separate SM events and, thus, the direct identification of multiple analytes can be readily achieved. These filters are expected to have a direct impact in the design and fabrication of sensors for continuous-flow monitoring in fields such as environmental pollution, homeland security, or biodetection.

Acknowledgment. M.A.C.-D. and R.A.A.-P. acknowledge the IPP (Xunta de Galicia, Spain) and RyC (MEC, Spain) programs, respectively. This work was funded by the Spanish Ministerio de Ciencia e Innovacion (Grants MAT2007-62696 and MAT2008-05755) and the Xunta de Galicia (Grants PGIDIT06TMT31402PR and 08TMT008314PR). We thank A. Benedetti (CACTI, Universidade de Vigo) for carrying out the FIB sample preparation.

REFERENCES AND NOTES

- (1) Aroca, R. F. *Surface Enhanced Vibrational Spectroscopy*; Wiley: New York, 2006.

- (2) Alvarez-Puebla, R. A.; Liz-Marzán, L. M. *Small* **2010**, DOI: 10.1002/smll.200901820
- (3) Rodríguez-Lorenzo, L.; Alvarez-Puebla, R. A.; Pastoriza-Santos, I.; Mazzucco, S.; Stephan, O.; Kociak, M.; Liz-Marzán, L. M.; García de Abajo, F. J. *J. Am. Chem. Soc.* **2009**, *131*, 4616–4618.
- (4) Qian, X. M.; Nie, S. M. *Chem. Soc. Rev.* **2008**, *37*, 912–920.
- (5) Kneipp, J.; Kneipp, H.; Kneipp, K. *Chem. Soc. Rev.* **2008**, *37*, 1052–1060.
- (6) Camden, J. P.; Dieringer, J. A.; Wang, Y.; Masiello, D. J.; Marks, L. D.; Schatz, G. C.; Van Duyne, R. P. *J. Am. Chem. Soc.* **2008**, *130*, 12616–12617.
- (7) Brus, L. *Acc. Chem. Res.* **2008**, *41*, 1742–1749.
- (8) Goulet, P. J. G.; Pieczonka, N. P. W.; Aroca, R. F. *Anal. Chem.* **2003**, *75*, 1918–1923.
- (9) Constantino, C. J. L.; Lemma, T.; Antunes, P. A.; Aroca, R. *Anal. Chem.* **2001**, *73*, 3674–3678.
- (10) Doering, W. E.; Nie, S. *J. Phys. Chem. B* **2001**, *106*, 311–317.
- (11) Bosnick, K. A.; Jiang, J.; Brus, L. E. *J. Phys. Chem. B* **2002**, *106*, 8096–8099.
- (12) Alvarez-Puebla, R. A.; Dos Santos, D. S.; Aroca, R. F. *Analyst* **2004**, *129*, 1251–1256.
- (13) Sanles-Sobrido, M.; Correa-Duarte, M. A.; Carregal-Romero, S.; Rodríguez-González, B.; Alvarez-Puebla, R. A.; Herves, P.; Liz-Marzán, L. M. *Chem. Mater.* **2009**, *21*, 1531–1535.
- (14) Taladriz-Blanco, P.; Rodríguez-Lorenzo, L.; Sanles-Sobrido, M.; Herves, P.; Correa-Duarte, M. A.; Alvarez-Puebla, R. A.; Liz-Marzán, L. M. *ACS Appl. Mater. Interfaces* **2009**, *1*, 56–59.
- (15) Abalde-Cela, S.; Ho, S.; Rodríguez-González, B.; Correa-Duarte, M. A.; Álvarez-Puebla, R. A.; Liz-Marzán, L. M.; Kotov, N. A. *Angew. Chem., Int. Ed.* **2009**, *48*, 5326–5329.
- (16) Sanchez-Cortes, S.; Garcia-Ramos, J. V.; Morcillo, G.; Tinti, A. *J. Colloid Interface Sci.* **1995**, *175*, 358–368.
- (17) Braun, G.; Pavel, I.; Morrill, A. R.; Seferos, D. S.; Bazan, G. C.; Reich, N. O.; Moskovits, M. *J. Am. Chem. Soc.* **2007**, *129*, 7760–7761.
- (18) Lee, S. J.; Morrill, A. R.; Moskovits, M. *J. Am. Chem. Soc.* **2006**, *128*, 2200–2201.
- (19) Le Ru, E. C.; Meyer, M.; Blackie, E.; Etchegoin, P. G. *J. Raman Spectrosc.* **2008**, *39*, 1127–1134.
- (20) Etchegoin, P.; Cohen, L. F.; Hartigan, H.; Brown, R. J. C.; Milton, M. J. T.; Gallop, J. C. *J. Chem. Phys.* **2003**, *119*, 5281–5289.
- (21) Pieczonka, N. P. W.; Aroca, R. F. *Chem. Soc. Rev.* **2008**, *37*, 946–954.
- (22) Goulet, P. J. G.; Aroca, R. F. *Anal. Chem.* **2007**, *79*, 2728–2734.
- (23) Etchegoin, P. G.; Le Ru, E. C.; Meyer, M. *J. Am. Chem. Soc.* **2009**, *131*, 2713–2716.
- (24) Etchegoin, P. G.; Meyer, M.; Blackie, E.; Le Ru, E. C. *Anal. Chem.* **2007**, *79*, 8411–8415.

AM9008715